

# Manipulating Si(100) at 5 K using qPlus frequency modulated atomic force microscopy: Role of defects and dynamics in the mechanical switching of atoms

A. Sweetman,<sup>1,\*</sup> S. Jarvis,<sup>1</sup> R. Danza,<sup>1</sup> J. Bamidele,<sup>2</sup> L. Kantorovich,<sup>2</sup> and P. Moriarty<sup>1</sup>

<sup>1</sup>*School of Physics and Astronomy, University of Nottingham, Nottingham NG7 2RD, United Kingdom*

<sup>2</sup>*Department of Physics, King's College London, The Strand, London WC2R 2LS, United Kingdom*

(Received 8 April 2011; revised manuscript received 11 July 2011; published 25 August 2011)

We use small-amplitude qPlus frequency modulated atomic force microscopy (FM-AFM), at 5 K, to investigate the atomic-scale mechanical stability of the Si(100) surface. By operating at zero applied bias the effect of tunneling electrons is eliminated, demonstrating that surface manipulation can be performed by solely mechanical means. Striking differences in surface response are observed between different regions of the surface, most likely due to variations in strain associated with the presence of surface defects. We investigate the variation in local energy surface by *ab initio* simulation, and comment on the dynamics observed during force spectroscopy.

DOI: [10.1103/PhysRevB.84.085426](https://doi.org/10.1103/PhysRevB.84.085426)

PACS number(s): 81.16.Ta, 68.35.Md, 68.37.Ps, 81.05.Cy

## I. INTRODUCTION

Frequency modulated atomic force microscopy (FM-AFM), operating in the constant-amplitude mode in ultrahigh vacuum (UHV), has developed into a widely used tool that provides unparalleled measurement, and manipulation capabilities at the atomic scale. Since first demonstrating true atomic resolution on reactive surfaces,<sup>1</sup> FM-AFM has been instrumental in the field of nanoscience, providing direct measurement of chemical forces<sup>2</sup> and enabling atomic manipulation on semiconducting,<sup>3–5</sup> metallic,<sup>6</sup> and insulating<sup>7,8</sup> surfaces. This is in addition to examples of subatomic<sup>9</sup> and striking submolecular<sup>10</sup> resolution.

Unlike the scanning tunneling microscope (STM), FM-AFM exploits the shift in resonant frequency,  $\Delta f$ , of a cantilever due to the interaction between tip and sample as its feedback parameter. In addition to enabling operation on insulating samples this critically allows measurement of the force between tip and sample during imaging and manipulation. Typically, however, a bias is applied to tip or sample in order to null out the contact potential difference (CPD) and hence eliminate the long-range electrostatic (ES) force. This applied bias has recently been used to facilitate the simultaneous mapping of force and tunnel current,<sup>11,12</sup> and the determination of the direct relationship between force and tunnel current at low bias.<sup>13</sup> Nonetheless, care must be taken that the applied bias does not modify the tip-sample interaction in an unexpected fashion. Indeed, the role of the applied bias in determining the observed topography on even well understood surfaces such as Si(111) is still not conclusively resolved.<sup>14–17</sup> Furthermore, some systems are especially sensitive to the influence of tunneling electrons. A prime example is the Si(100) surface, which has been the subject of considerable debate due to conflicting STM and low energy electron diffraction (LEED) studies (see, for example, Uda *et al.*<sup>18</sup> for a review).

The Si(100) surface at low temperature has presented a significant challenge to the surface science and nanoscience communities, primarily due to the delicate energy balance associated with its ground state, and its relative instability. Although it is now accepted that below  $\sim 120$  K the surface assumes the buckled  $c(4 \times 2)$  ground-state structure<sup>18–23</sup> [see Fig. 1(e) for schematic representations of the surface buckling

structure], the interpretation of scanning probe microscope (SPM) images can still remain challenging. For STM in particular, effects related to bulk and surface state contributions to the local density of states (LDOS) or dimer flipping induced by tunnel current injection<sup>20–22,24</sup> can result in an apparent  $p(2 \times 1)$  periodicity. In previous low-temperature FM-AFM studies the appearance of the apparent  $p(2 \times 1)$  phase was also observed and assigned to dimer flipping induced by the chemical bond between the tip and surface atoms.<sup>23</sup> These earlier studies, however, did not conclusively eliminate the possibility of additional tunnel-current-induced flipping, due to the bias used to null out the CPD.<sup>23</sup>

It has been shown that tunnel current injection can provide a powerful tool for phason [phase defect; see Fig. 1(e)] manipulation on both Si(100) and the related Ge(100) surface.<sup>20,25,26</sup> Critically, these tunneling-electron-derived effects are directly influenced or controlled by the complicated electronic structure of the surface and most likely depend on dopant type.<sup>22</sup> Recent STM and combined STM-AFM studies on Si(111)<sup>12,27</sup> have demonstrated not only that the dependence of tunnel current on tip-sample separation can become nonexponential at close approach, but also that peak tunnel currents during combined STM-AFM studies can be more than an order of magnitude higher than those in conventional STM studies.

We recently demonstrated atomically precise manipulation of the Si(100) surface by solely mechanical means, by operating a qPlus FM-AFM at zero applied bias.<sup>28</sup> Here, we report details of the tip-surface dynamics during manipulation, as well as discussing the variation in surface stability due to the influence of defects and step edges. We confirm that the energy balance of the surface is strongly influenced by the local environment, as has been previously reported in STM studies,<sup>29</sup> and that interpreting the tip-surface dynamics during FM-AFM manipulation of the Si(100) surface still provides a considerable challenge for state-of-the-art scanning probe and theoretical techniques.

## II. METHODS

### A. Experiments

All experiments were performed using a commercial (Omicron Nanotechnology GmbH) qPlus FM-AFM/STM,

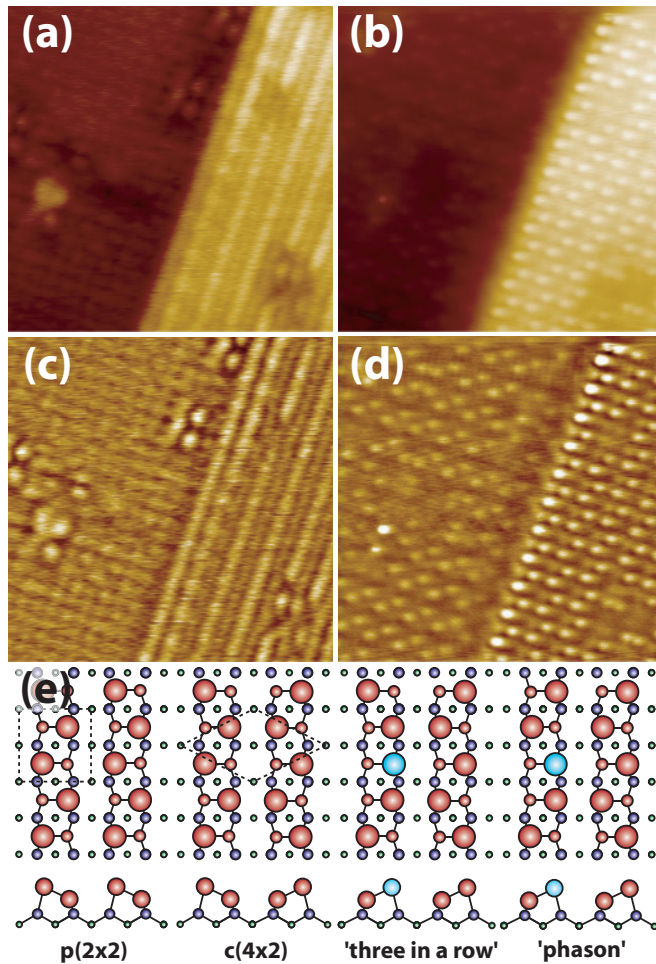


FIG. 1. (Color online) (a) Constant  $\langle I_t \rangle$  dSTM image of step edge on Si(100) at 5 K.  $V_{\text{gap}} = +2$  V;  $\langle I_t \rangle = 100$  pA;  $A_0 = 250$  pm. (b) Constant  $\Delta f$  FM-AFM image of the same region  $\Delta f = -17.6$  Hz;  $A_0 = 250$  pm;  $V_{\text{gap}} = 0$  V. (c) and (d) High pass filtered images of (a) and (b) respectively. The dSTM image shows significant nonlocal contributions (see main text). Zero-bias FM-AFM imaging shows the buckled  $c(4 \times 2)/p(2 \times 2)$  reconstructions on both terraces. (e) Schematics showing the  $p(2 \times 2)$  and  $c(4 \times 2)$  reconstructions. A single dimer flip from the  $c(4 \times 2)$  would result in a “three-in-a-row” structure (never observed experimentally). A phason (phase defect) results in a switch between in-phase [ $c(4 \times 2)$ ] and out-of-phase [ $p(2 \times 2)$ ] buckling.

operating in ultrahigh vacuum (UHV) (base pressure  $5 \times 10^{-11}$  mbar or better), in a LHe/LN<sub>2</sub> bath cryostat (sample temperature approximately 5 K for cooling with LHe, 77 K with LN<sub>2</sub>). We used boron-doped (1 m $\Omega$ cm) Si(100) surfaces which were prepared in UHV by standard methods (flash heating to  $\sim 1200$  °C; rapid cooling to  $\sim 900$  °C; slow cooling to room temperature) before transfer into the low-temperature cryostat. After preparation, we checked the Si(100) surface reconstruction by conventional STM using a qPlus sensor before beginning FM-AFM experiments. We used commercial qPlus sensors (Omicron) with an electrochemically etched tungsten wire attached to one tine of the tuning fork. These were introduced into the scan head without further preparation (e.g., e-beam heating or argon sputtering). Calibration of the

quality factor and stiffness are described in detail elsewhere.<sup>28</sup> Briefly, we recorded  $Q$  factors of between 1000 and 50 000 at 5 K with resonance frequencies of between 22 and 25 kHz, and tuning fork stiffness of  $k = 2600$  N/m ( $\pm 400$  N/m).<sup>28</sup>

The sensors were prepared using standard STM techniques (e.g., voltage pulsing, controlled tip crashes) until atomic resolution was obtained. We then performed dynamic STM (dSTM) (i.e., tunnel-current-based feedback with an oscillating tip) and transferred to constant  $\Delta f$  (i.e., FM-AFM) feedback and subsequently reduced the tip bias to 0 V. We would then increase the frequency shift set point until we began to observe atomic resolution. In some cases we immediately obtained atomic resolution after transferring from dSTM; in other cases it was necessary to perform small controlled contacts with the surface to alter the tip state. As a consequence of our tip preparation techniques (and evidence from scanning electron microscope measurements on similarly prepared STM tips<sup>28</sup>) we expect the apex of the tip to be silicon rather than tungsten terminated. The reduction of the tip bias to 0 V is essential both in order to remove the possibility of electronic crosstalk from the  $I_t$  channel<sup>30</sup> and, critically, to also eliminate the effect of tunneling electrons. As a consequence, we do not null out any contact potential difference (CPD) between tip and surface, and as such a large electrostatic background may be present. Nonetheless, we routinely observed atomic resolution even with relatively blunt tips (e.g., tips that experienced surface indentations in excess of 1000 nm could still produce atomic resolution), most likely because operating with small oscillation amplitudes increases our sensitivity to the short-range chemical force.<sup>31–33</sup>

## B. Simulations

We simulated the interaction between the silicon surface and a silicon tip cluster by *ab initio* density functional theory (DFT) as implemented in the SIESTA code.<sup>35</sup> Two tip clusters were used, a standard Si(111)-type tip and a larger dimer-terminated cluster, as described elsewhere.<sup>28</sup> We used a double-zeta polarized basis set giving 13 orbitals to describe the valence electrons on every silicon atom. Calculations were performed with the generalized gradient approximation (GGA) Perdew-Burke-Ernzerhof (PBE) density functional and norm-conserving pseudopotentials. Typically, atomic relaxation was considered complete when forces on atoms were not larger than 0.01 eV/Å.

In all simulations a 6-layer slab model was used with 16 surface dimers arranged as 2 rows, each 8 dimers in length. Hydrogen atoms were used to terminate the Si bonds on the lower side of the slab and were kept fixed, along with the bottom two layers of silicon, to simulate the missing bulk. We used a large slab size to provide reasonable isolation of the target atoms in order to reduce finite-size effects due to periodic boundary conditions. Atoms are only manipulated within a single row, such that there is always a single unaffected dimer row between the manipulated row and its periodically repeated counterparts. In addition, the length of each row was chosen to reduce any effect due to long-range surface relaxations along the rows. For example, when modeling a phason pair (two adjacent phasons, four dimers in length), four other dimers, in a standard  $c(4 \times 2)$  buckling configuration, separate the

structure from the repeat of the phason unit. Because of the cell sizes used, only the  $\Gamma$  point was employed in sampling the Brillouin zone in all of our simulations.

To estimate the energy barriers between different configurations we performed nudged elastic band (NEB) calculations, using SIESTA to calculate the total energies. In our NEB calculations we modeled the evolution of the energy band corresponding to the minimum energy path between the  $c(4 \times 2)$  and phason pair structures in the presence of a silicon tip cluster. The NEB method allowed us to calculate the dimer atom positions and energy barriers associated with the minimum energy pathway between two states. Initially, the start and end points on the band were relaxed and the atomic positions along the band were obtained by a linear interpolation with 17 images in each band. For the data presented in this paper the band was then relaxed until the energies of the images varied by less than 0.01 eV and the force less than 0.1 eV/Å.

### III. RESULTS

Our results are divided into two broad categories. First, we discuss imaging of the Si(100) surface and variation in the surface stability observed during scanning, comparing the data to simulated variations in surface stability. Second, we investigate the variations in tip-surface dynamics during site-specific atomic switching events induced by  $\Delta f(z)$  spectroscopy and attempt to elucidate the dynamics by comparison to simulated force spectroscopy.

#### A. Local variation in surface stability during scanning

During our dSTM experiments we observed a strong influence of tip bias and tunnel current set point on the imaging process, as previously reported. The observed surface structure can change as a result of tunnel current injection, tunneling into nonlocalized surface and bulk states and charging at defects.<sup>20–22,24,36,37</sup> However, once we transition to zero-bias FM-AFM we always observe buckled dimers in the  $p(2 \times 2)/c(4 \times 2)$  configuration on both terraces (Fig. 1 shows a typical transition). In this instance we note the dSTM image shows significant influence from the tip state as the upper and lower terraces show different contrast [ $p(2 \times 1)$  on the lower terrace and rows on the upper terrace]. Given the relatively high bias applied during the dSTM imaging (+2 V), there are likely to be significant contributions from the bulk-like states of the surface and tip, and elucidating the origin of this contrast is beyond the scope of this paper. Importantly, this influence is not apparent in the FM-AFM image, highlighting the different origin of the contrast in each imaging mode.

It is well known that the buckling of the silicon dimers can be “pinned,” even at room temperature, by features such as defects, adsorbed molecules, or step edges due to their effect on the local strain along the surface. Consequently, the barrier for dimer flipping exhibits strong local variation.<sup>29,38,39</sup> Similarly, we found local variations in the propensity for dimers to flip under the influence of the tip at low temperatures. This is clearly demonstrated in Fig. 2 (see also movie S1<sup>30</sup>), which shows the transition from the buckled structure to the apparent symmetric  $p(2 \times 1)$  periodicity as the  $\Delta f$  set point is increased.<sup>23</sup> In particular in Fig. 2(f) the apparent  $p(2 \times 1)$

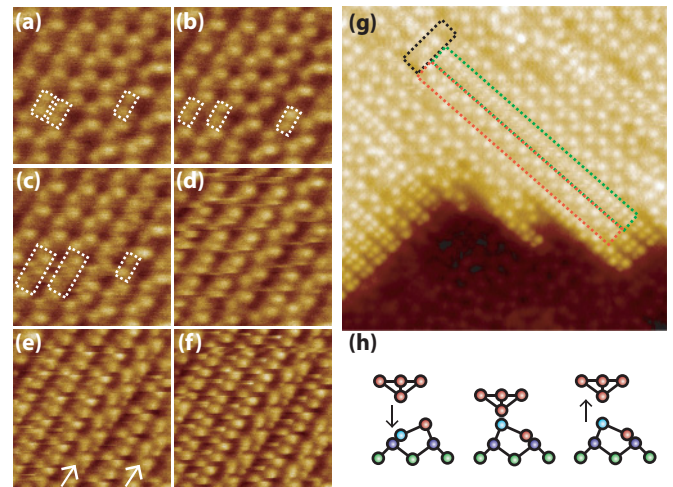


FIG. 2. (Color online) Scan-induced phason manipulation and  $c(4 \times 2)$ -to- $p(2 \times 1)$  transition. (a) FM-AFM image showing an unperturbed buckled surface structure and three “native” phason defects (highlighted).  $\Delta f = -26$  Hz;  $A_0 = 100$  pm;  $V_{\text{gap}} = 0$  V. (b)  $\Delta f = -27$  Hz. At higher set points we observe scan-induced phason motion, as previously reported (Ref. 28). (c)  $\Delta f = -28$  Hz. At still higher set points the position of some of the phasons becomes difficult to identify (larger highlighted regions). (d)  $\Delta f = -29$  Hz. “Intermittent” imaging. It is now likely that dimers are being flipped from the buckled state in addition to scan-induced phason motion. Clear “slicing” is evident in a number of rows. (e)  $\Delta f = -31$  Hz. At high set points some rows now show the apparent  $p(2 \times 1)$  phase while some remain buckled (indicated by white arrows). (f)  $\Delta f = -34$  Hz. The highest set point at which we could reliably image with this tip—see main text for details. (g) Scan taken with a different tip at 77 K and a small bias voltage illustrating long-range differences in dimer stability.  $\Delta f = -40$  Hz;  $A_0 = 100$  pm;  $V_{\text{gap}} \sim 10$  mV. A boron ad-dimer defect (Ref. 34) (black box) appears to reduce the barrier for dimer flipping in the row highlighted by the green box. An adjacent row (red box) images as a stable buckled structure. The apparent effect of the defect on dimer stability extends over almost 30 dimers. Note that due to the small bias we cannot exclude tunnel-current-induced flipping in this instance ( $\langle I_t \rangle$  during imaging  $\sim 2$  pA). (h) Cartoon representation of tip-induced dimer flipping.

phase is clear in a number of rows. Nonetheless, two rows still show a buckled structure, indicating that even under the same imaging conditions some dimers are less likely to be perturbed by the tip-sample interaction. We note that the rows remaining buckled have an asymmetric appearance, most likely due to an asymmetric tip apex. Figure 2(g) demonstrates a clear example of the nonlocal effect that defects can exert on dimer stability. A previous study reported that strain at step edges resulted in a lowering of the surface stability on the lower terrace and an apparent  $p(2 \times 1)$  periodicity during FM-AFM imaging.<sup>40</sup> We, however, always observed buckling on both terraces at low set point, with no apparent preference for scan-induced phason motion (see below) on either terrace. This variance may be due to our elimination of the effect of tunneling electrons, or possibly variation in defect density close to the scan region.

When the scan-induced  $p(2 \times 1)$  periodicity is observed we note that determining the actual structure of the surface (at a given instant) is likely to be nontrivial. This is primarily

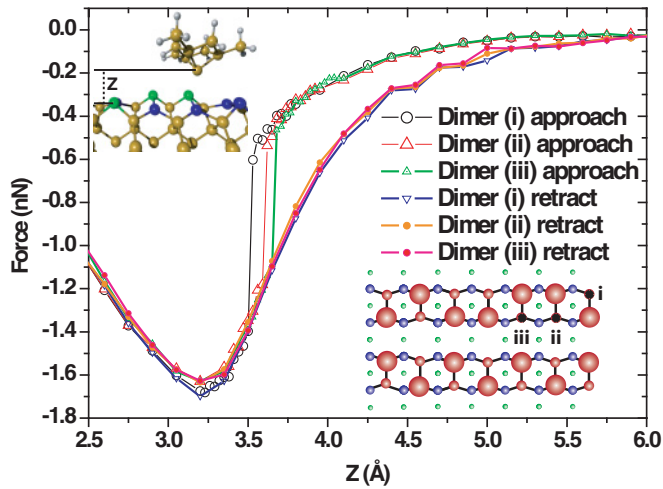


FIG. 3. (Color online) Variation in threshold force needed to flip a dimer during simulated force spectroscopy around a phason pair. The threshold force is reduced for dimers (iii) and (ii), but dimer (i) has approximately the same threshold as a dimer in  $c(4 \times 2)$  configuration. Insets: Top left, rendered representation of tip-sample positioning; bottom right, schematic of part of the simulated cell showing spectroscopy locations.

due to the difficulty in distinguishing between a number of different cases that might result in a  $p(2 \times 1)$  periodicity. During FM-AFM spectroscopy we have shown that phasons are injected in pairs if the tip approaches close enough to the “down” atom of a dimer<sup>28</sup> [that is, we only observe *correlated* flips on the  $c(4 \times 2)$  surface]. However, we also note that native phasons are less stable than the buckled surface. Therefore, as expected, we observe induced phason motion before we see flipping in pristine buckled rows. However, once the threshold for phason injection is reached, it will be difficult to distinguish between subsequent (mechanically driven) phason motion and further phason pair injection within the row. Any long-range relaxations or variation in surface stress will only complicate the interpretation of the images. We also note that the same difficulty in interpretation will be true for STM images showing tunnel-current-induced dimer flipping.

We investigated the variability in surface stability via a combination of simulated DFT force spectroscopy and NEB energy barrier calculations. The simulations are broken down into two approaches. In the first we analyzed the variation in the force threshold to “flip” a dimer during force spectroscopy over the “down” atom of a dimer in the presence of both dimer buckling (i.e., phase related) and structural (i.e., missing dimer) defects. In the second we investigated the variation in the potential energy surface to transition from a pristine buckled surface to a phason pair structure in the presence of the tip under induced surface strain.

Figures 3 and 4 show the calculated variation in threshold force around a phason pair (buckling) defect and a single dimer vacancy (1DV) structural defect, respectively. As in previous studies<sup>41</sup> simulated force spectroscopy resulted in a single dimer flip only, which, depending on the initial configuration, resulted in structures which were never observed experimentally (e.g., “three in a row”). However, in both cases we observe differences in the force threshold compared to

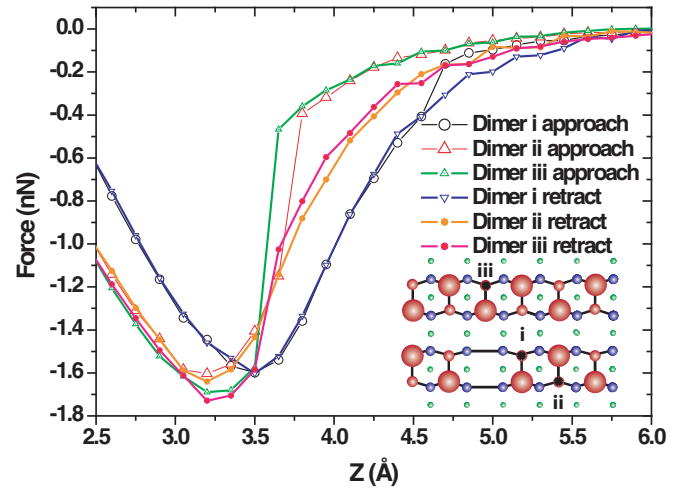


FIG. 4. (Color online) Variation in threshold force needed to flip a dimer during simulated force spectroscopy around a dimer vacancy defect. The threshold force is significantly reduced for dimer (i) and slightly reduced for (ii). Dimer (iii) has approximately the same threshold as a dimer in  $c(4 \times 2)$  configuration. Inset: Schematic of part of the simulated cell showing spectroscopy locations.

a pristine surface, similar to our experimental observations which suggest that the force threshold to flip a dimer varies depending on the local surface configuration.<sup>28</sup>

In our NEB simulations we adopted an alternative approach, with the aim of simulating the long-range strain effect of a distant defect, by artificially introducing a lattice mismatch on the lower atoms of our simulated cell (as previously described for molecular dynamics simulations<sup>28</sup>). The spacing of the fixed atoms was changed by a small amount (0.3 Å) along the direction of the rows, and, after allowing the lattice to relax, we explored the energy barriers to transit from the buckled surface to a phason pair structure with the tip at the threshold position to flip. We observed a drop in the barrier to transit from the “three in a row” to the phason pair (Fig. 5) upon both artificial contraction and expansion of the lattice spacing. We note that although the subsurface displacement is moderate, the response at the surface is relatively small ( $\sim 0.1$  Å), of order, or smaller than, reported surface strains (0.1–0.8 Å) induced by surface defects.<sup>40,42</sup> Indeed, strains of this magnitude would be of the same order as the noise in the measurement during FM-AFM imaging ( $\sim 0.1$  Å).<sup>40,42</sup> It is possible that some defect structures and the resulting strain fields may lower the barrier still further, but an extensive theoretical investigation of the effect of different defects on the PES, with the prerequisite large simulation cells, is beyond the scope of this paper.

Consequently we find that FM-AFM is able to directly probe the stability of the Si(100) surface structure with atomic precision, and we find qualitative agreement with our simulations in that both structural and phase defects (and long-range strain) directly alter the stability of the dimer buckling. It seems likely that such experiments could provide a direct quantitative way of measuring strain fields, which may have uses in determining the effect on a surface as a result of atomic-scale damage, substitutional defects, or implantation experiments. Combining such techniques with STM could also provide a method of directly visualizing the link between

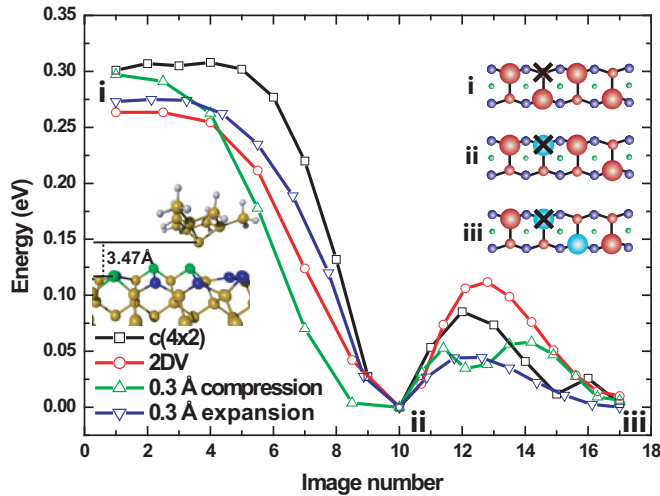


FIG. 5. (Color online) NEB-calculated energy profiles associated with the transition from a  $c(4 \times 2)$  structure [position (i)] to a phason pair configuration [position (iii)] for different surfaces with a Si(111) type tip positioned laterally over the lower atom of a dimer, with the terminating atom at a height of  $3.47 \text{ \AA}$  (defined from the vertical position of the upper dimer atom). At this tip-sample separation, the barrier for the transition to an intermediate three-in-a-row state [position (ii)]—never observed experimentally—collapses in all cases. However, a substantial energy barrier ( $\sim 80 \text{ meV}$ ) remains to transit to the phason pair structure for the pristine surface (black squares). Introducing a two-dimer-vacancy (2DV) defect (red circles) increases the energy barrier between the three-in-a-row and phason pair to  $\sim 110 \text{ meV}$  (Ref. 28), while a small subsurface compression (green upward-pointing triangles) or expansion (blue downward-pointing triangles) reduces the barrier ( $\sim 60 \text{ meV}$  and  $\sim 45 \text{ meV}$ , respectively). Each curve has been offset to normalize the position of the three-in-a-row state to aid comparison of the barriers. Insets: Bottom left, rendered representation of tip-sample positioning during NEB; top right, schematic representation of surface states at three positions on the energy profile. Black cross indicates lateral position of the tip.

physical strain and resulting deformation of the electronic structure of the material.

### B. Atomically precise switching: Tip-sample dynamics and spectral signatures

Although we have previously shown that FM-AFM force spectroscopy at 5 K allows for controlled, reversible phason pair injection and atomically precise mechanically driven phason motion,<sup>28</sup> we also observe a high proportion of *failed* attempts when attempting to flip dimers from the  $c(4 \times 2)/p(2 \times 2)$  structure. In these instances we would perform the same procedure as for a normal flip, but the  $\Delta f$  spectra would demonstrate different features (see next subsection) and there would be no change in the structure of the surface after spectrum acquisition had completed. From the spectra it is clear that we are perturbing the surface [i.e., the lower atom of the dimer is moving toward the tip; see Fig. 2(b)], but that the new configuration is not stable and the surface relaxes back into its original configuration once the tip has retracted. There are two critical variables that may

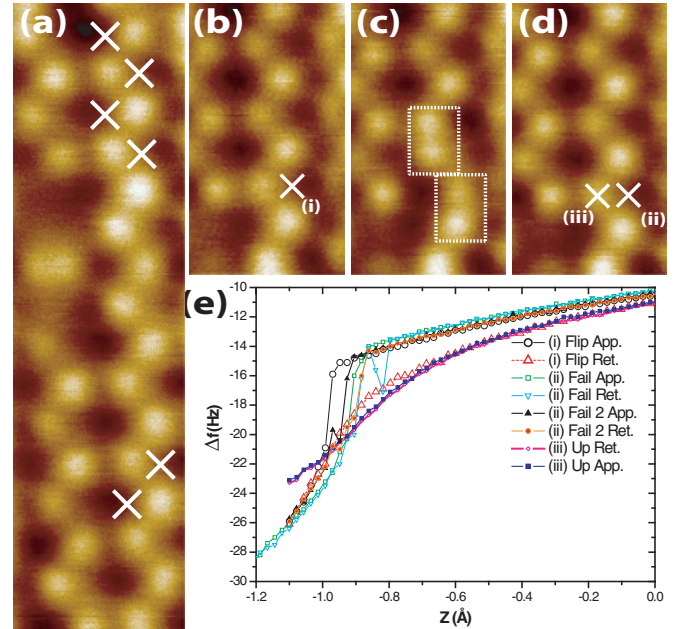


FIG. 6. (Color online) (a) Unsuccessful attempts to flip a dimer in the  $c(4 \times 2)/p(2 \times 2)$  buckled structure. Each white cross indicates the location of a  $\Delta f$  spectroscopy point. In this area every attempt to flip a dimer failed. (b) Successful and failed flips on the same dimer (in a different region of the surface): Initial  $c(4 \times 2)/p(2 \times 2)$  buckled surface configuration. A spectroscopy point was performed at (i) to generate a phason pair. (c) Configuration after spectroscopy, showing phason pair structure. (d) The  $c(4 \times 2)/p(2 \times 2)$  structure was restored and  $\Delta f$  spectroscopy was twice attempted on the  $c(4 \times 2)/p(2 \times 2)$  buckled structure in the same location (ii). Neither attempt produced a phason pair. Subsequently, a spectrum was taken over the “up” atom of the same dimer (iii). (e) Spectra from (b)–(d). (i) shows clear hysteresis (approach over down atom, flip, and retract over up atom). Subsequent attempts (ii) show unstable transitions and subsequent retract over a “down” atom, indicating failed flips.

influence the stability of the created structure—the precise tip position and the local variability of the surface.

As demonstrated in the previous section and in previous work,<sup>28,29</sup> there is clearly a variability in surface stability due to the influence of defects and step edges. Consequently, we find that in some regions numerous force spectroscopy points could be performed, without causing the formation of a phason pair [Fig. 6(a)]. However, and intriguingly, we also observed instances where we successfully injected a phason pair, removed the phason pair, and were then subsequently unable to inject a phason pair *in the same location* [Figs. 6(b)–6(d)]. Critically, it appears that the local surface configuration (within our scan window) was unaltered, and therefore arguments related to differences in the surface strain cannot completely explain our observations.

As such, other factors that may influence the probability of successful phason pair injection must be considered. Consequently we investigated the effect of lateral tip displacement on the chemical bonding force between tip and sample. It is self-evident that if the tip is positioned too far from the “down” atom location, very little bonding will result. However, in order to provide insight into the “failed flips,” the simulations must simultaneously demonstrate significant

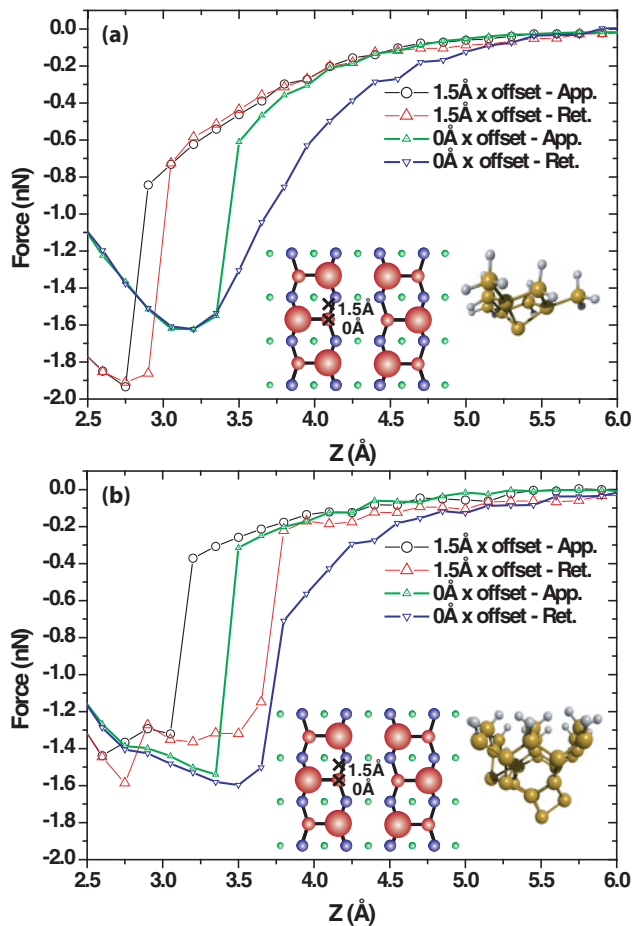


FIG. 7. (Color online) Simulated spectroscopy with laterally displaced tips. (a) Spectroscopy performed with Si(111)-type tip directly over a down atom (0 Å offset) and offset by 1.5 Å. (b) Spectroscopy performed with dimer-terminated tip directly over a down atom (0 Å offset) and offset by 1.5 Å. In both cases spectroscopy directly over the atom resulted in a flip, while the offset spectroscopy resulted in a failed flip. Insets: Location of spectroscopy points, marked with a cross (left) and rendered representations of the tip structures (right).

chemical bonding (i.e., a sharp jump in force resulting from the dimer changing configuration), but not result in a permanent change in surface configuration after the tip is withdrawn. We found that for simulated spectroscopy with idealized tips certain lateral displacements reproduced this behavior (Fig. 7). In these instances it appears that the dimer changes configuration in response to the presence of the tip, but the change in buckling angle is reduced, with the dimer assuming an almost symmetric configuration while bonded to the tip. Once the tip is withdrawn the symmetric dimer relaxes back into its original buckled configuration. Subsequently, it is plausible that at least some of the failed flips we observe could be a combination of surface variability and a lack of precision in lateral positioning. It must be emphasized that in these cases the simulated spectroscopy indicates a failure to reach the “3 in a row” configuration. These simulations do not address instances where the “3 in a row” may be formed, but the surface does not subsequently transit to the phason pair configuration. Our DFT simulations suggest that

if the “3 in a row” structure is reached during spectroscopy, it remains stable even when the tip is withdrawn. In contrast, the results of NEB calculations, molecular dynamics (MD) simulations,<sup>28</sup> and experiment suggest it will relax back to the buckled structure in the absence of the tip, and, as such, any flip that does not result in a transition to a phason pair (or other stable structure) will also result in a failed flip.

In order to better understand the dynamics during flip attempts, we performed an analysis of the spectroscopy data acquired during  $\Delta f(z)$  spectroscopy experiments. During our investigation we noted several different characteristic  $\Delta f(z)$  curves that acted as reliable “signatures” for different classes of flip event. These signatures appear to result from differences in the dynamics occurring during the spectroscopy events. First, we note that spectra taken over an “up” atom produce a smoothly varying  $\Delta f(z)$  curve, as has been seen for previous FM-AFM investigations of Si(111) surfaces.<sup>2</sup> Importantly, these curves show very similar profiles to the retract curves taken during successful flip attempts, strongly indicating that after a flip the tip is retracting over an “up” atom. Here we classify our observations into four broad categories. Figure 8 shows representative examples of each type.

### 1. Successful flip type (i)

In the case of a normal dimer flip, we typically observe a smooth increase in  $\Delta f$  up to a threshold, followed by a sudden jump. After this jump the  $\Delta f$  curve would follow a different path (which it retraced on retract), resulting in hysteresis in the  $\Delta f(z)$  curve [Fig. 8(a)]. We interpret this sudden jump in  $\Delta f$  as being due to the lower atom of the dimer “jumping up” into closer proximity to the tip, and the different retract curve as being caused by the tip retracting over what is now an “up” atom. This is qualitatively similar to the force-distance curves from simulated spectroscopy demonstrating a successful dimer flip.<sup>28</sup>

### 2. Unsuccessful flip type (i)

In these instances there is a sharp change in  $\Delta f$  on approach indicating the dimer has flipped, and on the retract  $\Delta f$  follows a different path as for a successful flip. However, at some point on the retract curve (but clearly at a different point in  $z$  from the original sharp change) we see the  $\Delta f$  signal jump back to the same value it had on the approach curve. This appears to indicate that the “up” atom state is, in these instances, temporarily stabilized by the presence of the tip but unstable on retraction. A possible explanation is the dimer configuration not transitioning to the phason pair structure and remaining in the unstable three-in-a-row state, or not being pulled up sufficiently and remaining symmetric in the presence of the tip. The failure of the dimer to stay flipped indicates subtle variations in the dimer position and local strain may play a key role in stabilizing the dimer configuration. This appears qualitatively similar to simulations of a failed flip attempt with a laterally displaced, dimer-terminated, tip [Fig. 7(b)].

### 3. Unsuccessful flip type (ii)

In most cases an unsuccessful flip would result in a sharp increase in  $\Delta f$  (as for a successful flip), but then as the tip retracted we observed another sharp change in  $\Delta f$  (at almost

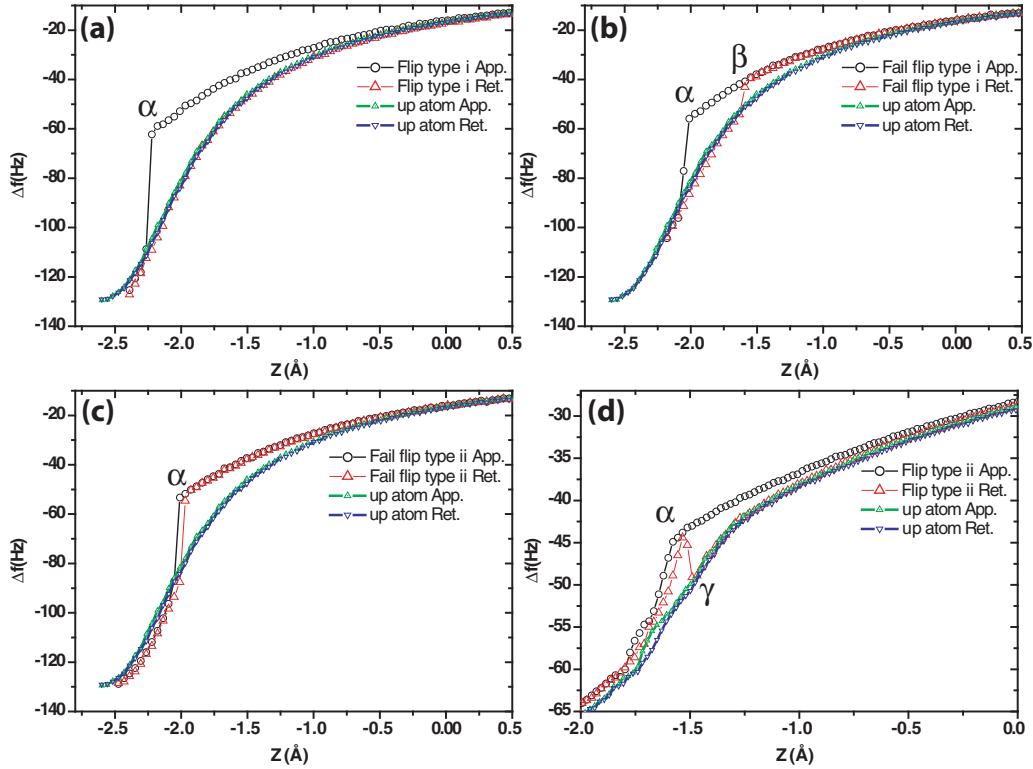


FIG. 8. (Color online) Representative examples of  $\Delta f(z)$  “signatures.” (a) to (c) were acquired using the same tip apex ( $A_0 = 50$  pm). (d) was acquired using a different tip apex and different parameters ( $A_0 = 250$  pm) as this type of event was comparatively rare. On each graph a  $\Delta f(z)$  curve taken over an “up” atom with the same tip is plotted to aid comparison with the retract  $\Delta f(z)$  curves. (a) Successful flip type (i), showing a smooth increase followed by a sudden discontinuity ( $\alpha$ ) and subsequent retract along a different path. The retract curve exhibits a strong similarity to the  $\Delta f(z)$  curve taken over an “up” atom. (b) Unsuccessful flip type (i). Similar behavior as shown in (a) except that on the retract a sudden jump back onto the approach curve is detected ( $\beta$ ), indicating that the atom under the tip has dropped back into a “down” state. (c) Unsuccessful flip type (ii). In this instance the jump on retract is in almost the same position as the initial jump, resulting in very little hysteresis in the  $\Delta f(z)$  curve. (d) Successful flip type (ii) taken from a different data set with a different long-range  $\Delta f(z)$  behavior. Here it appears that the flip has failed as the retract follows the same path as approach, but then suddenly jumps down onto the “up” atom curve ( $\gamma$ ).

the same  $z$  position) such that the  $\Delta f$  curve on the retract follows the same path as the approach. In these cases there is only a very small amount of hysteresis between the two paths. A simple interpretation of these events is that the down atom is pulled up, but is not stable without the presence of the tip, and as the tip leaves the surface the dimer simply drops back into its original configuration. This suggests that small variations in the potential energy surface may sometimes enable the system to go back from the three-in-a-row configuration to  $c(4 \times 2)$  even with the tip relatively close to the surface. In this instance the results closely resemble a simulated failed flip using a laterally displaced Si(111)-type tip [Fig. 7(a)].

#### 4. Successful flip type (ii)

Very rarely we would observe a jump on the approach and retract [as for a failed type (ii)], but subsequently during the retract we then see a further jump to a higher  $\Delta f$  value and subsequent different path during the rest of the retract. In these events it appears that the dimer flips, then drops back into its original configuration as the tip retracts, but then flips again and stays in the up position as the tip retracts. The tip-surface dynamics in these cases present a particular challenge as the

dimer appears to be flipping after the peak force has been reached and the tip is already retracting, suggestive of complex relaxations at the tip-surface interface.

#### C. Long-range relaxations during phason manipulation

Although we have demonstrated that the motion and positioning of phasons can be controlled with atomic precision by FM-AFM spectroscopy, we nonetheless also observe examples of unexpected long-range relaxations that hint at further complex intra-row coupling. We regularly observed two or more dimers flipping when we attempted to form “three (or more) in a row” structures, which, while not predicted in our simulations, may be expected if the surface is attempting to release a large quantity of locally induced strain. In addition, however, we also see long-range relaxations in locations where we would expect a *single* dimer flip to occur. What is striking in these examples is that the expected “target” structures are not only stable, but have been successfully formed in other regions during FM-AFM manipulation experiments. Consequently, it appears that variations in surface stability may affect not only our ability to create phason pairs, but also restrict our ability to maintain atomically precise control of

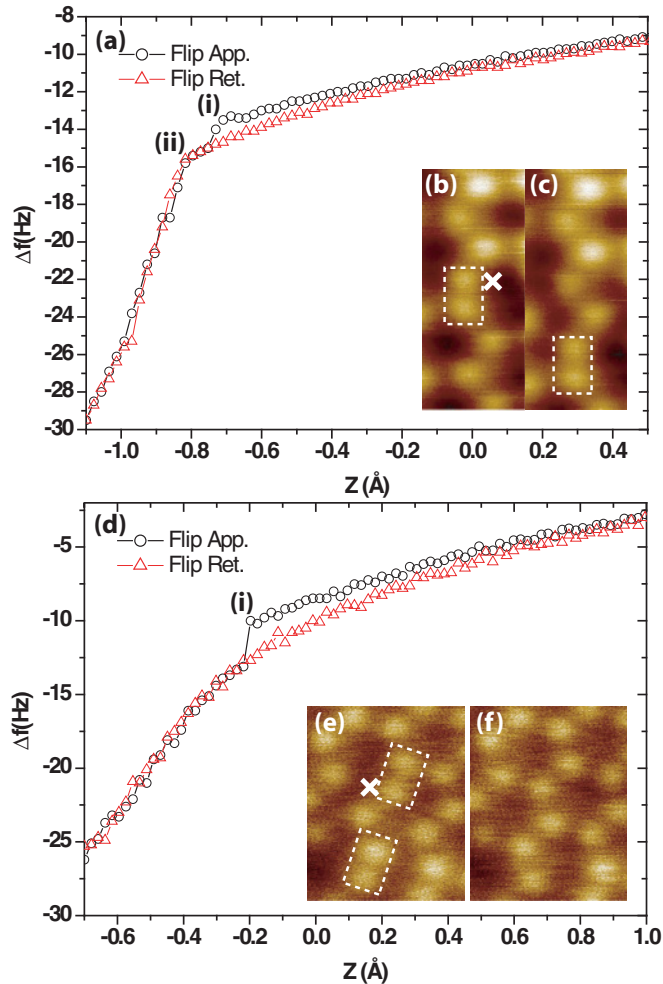


FIG. 9. (Color online) Long-range relaxations during attempted phason manipulation events. White crosses indicate location of  $\Delta f$  spectroscopy points. (a)  $\Delta f$  from attempted phason manipulation on an isolated phason. (b) Image showing surface before manipulation. The manipulation should flip the “down” atom under the tip and move the phason toward the top of the image. (c) Result of  $\Delta f$  spectroscopy. The targeted dimer is in its original configuration and the phason has moved two dimers toward the bottom of the image (i.e., two dimers have flipped in response to the original perturbation). In the  $\Delta f$  spectra a small jump is apparent [indicated by (i)] before a larger jump [indicated by (ii)]. On the retract the same path is followed (i.e., a “failed flip”), indicating the targeted atom has returned to its original position. The subsequent slight difference in the long-range behavior may be due to the changed state of the neighboring dimers. (d)  $\Delta f$  from attempted phason manipulation. The manipulation was intended to bring the two phasons together [i.e., a single dimer flip, as demonstrated previously (Ref. 28)]. A small jump is recorded (i). (e) Image showing surface before manipulation. (f) Result of  $\Delta f$  spectroscopy. Instead of flipping one dimer a long-range relaxation has occurred, with three dimers changing configuration, restoring the  $c(4 \times 2)/p(2 \times 2)$  structure.

phason motion. In Fig. 9(a) it appears that the neighboring dimer may be perturbed by the tip prior to the targeted dimer, despite positioning the tip with the same protocol as used in other, successful, manipulation attempts. In Fig. 9(b) the surface undergoes a relaxation to restore the  $c(4 \times 2)$

as we attempt to bring two phasons together, despite the target structure having been successfully fabricated in other regions of the surface.<sup>28</sup> In other instances (data not shown) we performed successful phason injection on the same dimer several times, but observed occasional long range changes. This, in conjunction with instances where we have been unable to inject phasons in the same location as a previous successful attempt (see Fig. 6), suggests either an extreme sensitivity to experimental parameters or a weakly nondeterministic process (see discussion).

#### D. Summary

From the spectra collected we propose that (in the absence of long-range relaxations) a simple protocol can be established for determining whether a given  $\Delta f(z)$  point has succeeded in changing the state of the dimer under the tip: (i) If a sharp change in  $\Delta f$  is detected on the approach curve this indicates that the “down” atom has jumped up toward the tip. (ii) If the  $\Delta f$  curve follows the path of an “up” atom on the retract without any further discontinuities this suggests that the tip is retracting over an “up” atom. There are cases where there are jumps between the two states, but the critical factor is whether the retract curve follows a different path (“up” atom) than the approach (“down” atom). In this case the dimer has changed configuration and the final configuration appears stable. If the  $\Delta f$  signal jumps back to the same path as the approach curve then this indicates that the dimer has dropped back to its original configuration and no permanent change has been made. We find significant variability in mechanical stability across the surface, but also note variation in dimer flips in the same location which cannot be explained by strain-induced variations in stability.

#### IV. DISCUSSION

Our simulations suggest plausible mechanisms that explain the experimentally observed variation in surface stability and the origin of the spectral signatures that we observe during manipulation events. Nonetheless, we emphasize that given the unknown structure of our experimental tip apex, and the uncertainty regarding local strain in the surface, these mechanisms can only be tentatively assigned. In particular we note that we estimate our lateral positioning error during experimental force spectroscopy to be  $\lesssim 1$  Å, much smaller than that required in our simulations to result in a failed flip. However, it may be that sub-Å changes in position are sufficient to cause failed flips for more complex tip structures or locally strained surfaces (such as in the vicinity of defects or step edges). Another important and intriguing possibility is that quantum mechanical tunneling could become important for dimer flip motion at low temperatures when the barriers are sufficiently small.<sup>43</sup> Although the silicon dimer has a relatively large mass, it has been shown that quantum effects can be important for objects as large as CO (Ref. 44) or Co (Ref. 45). Consequently, given the critical dependence of quantum mechanical tunneling on barrier height we cannot eliminate this as an explanation for some of the transitions we observe.

We note that confirming this hypothesis presents a significant experimental challenge as numerous aspects of the

experimental protocol need to be addressed. First, the lateral accuracy of the tip positioning could be greatly improved by the use of an atom-tracking protocol,<sup>46,47</sup> which has previously been shown to allow lateral positioning precision of  $\sim 0.1$  Å. Second, although we do not observe large variations in oscillation amplitude during spectroscopy, it could be that small variations on the order of a few percent somehow introduce enough variation between spectra to perturb the outcome, which might be eliminated by careful adjustment of the amplitude gain circuit and other experimental parameters. Lastly, any experiment investigating the statistical nature of the manipulation outcome will require a large number of manipulation attempts above the *same* dimer (due to the variations in propensity for flipping described above), at variable temperature (similar to previous SPM investigations of QM effects<sup>44</sup>), with the same tip structure, in order to be conclusive.

## V. CONCLUSION

We have confirmed that buckled dimers are the ground state of the Si(100) surface at low temperature in the absence of probe-induced effects.<sup>23</sup> Our experiments confirm the emergence of the apparent  $p(2 \times 1)$  periodicity at high set points due to mechanical dimer flipping, but reveal strong variations in surface stability on the atomic scale, which appear to originate from the effect of surface stress induced by defects and step edges. By operating at zero applied bias we are able to perform controlled atomic-scale manipulation of the buckling dimer configuration, but this ability is limited to certain surface regions. The variation in the surface stress can not only prevent manipulation, but also apparently

cause long-range relaxations, making atomic manipulation of the buckling configuration on the Si(100) surface critically dependent on the local and nonlocal environment of the target dimer. Our simulations accurately reproduce many qualitative aspects of the experiment, but we note that a significant theoretical effort, specifically with regard to the evolution of energy barriers between different states on large slabs (in the presence of defects), still needs to be made to address the role of dimer-dimer coupling during manipulation events. Further experiments, with improved lateral precision and at variable temperature, are needed to investigate whether the variation in outcome during manipulation over a single dimer is deterministic.

## ACKNOWLEDGMENTS

We acknowledge financial support from the Engineering and Physical Sciences Research Council (EPSRC) and the European Framework 6 training networks PATTERNS and NANOCAGE, J.B. in particular thanks EPSRC for studentship funding. We also acknowledge the support of the University of Nottingham High Performance Computing Facility, and computer time allocation on the HECTOR UK National Facility via the Material Chemistry consortium is greatly appreciated. We thank Gordon Shaw of the National Institute of Standards and Technology for the stiffness measurements on our qPlus sensors. Juergen Koeble and Andreas Bettac of Omicron Nanotechnology GmbH provided valuable advice and assistance with regard to our qPlus AFM system. We also thank Peter Beton, Oscar Custance, Neil Curson, Steven Schofield, and Joseph Stroschio for helpful comments and discussion.

\*adam.sweetman@nottingham.ac.uk

<sup>1</sup>F. J. Giessibl, *Science* **267**, 68 (1995).

<sup>2</sup>M. A. Lantz, H. J. Hug, R. Hoffmann, P. J. A. van Schendel, P. Kappenberger, S. Martin, A. Baratoff, and H. Guntherodt, *Science* **291**, 2580 (2001).

<sup>3</sup>N. Oyabu, O. Custance, I. Yi, Y. Sugawara, and S. Morita, *Phys. Rev. Lett.* **90**, 176102 (2003).

<sup>4</sup>Y. Sugimoto, M. Abe, S. Hirayama, N. Oyabu, O. Custance, and S. Morita, *Nature Mater.* **4**, 156 (2005).

<sup>5</sup>Y. Sugimoto, P. Pou, O. Custance, P. Jelinek, M. Abe, R. Perez, and S. Morita, *Science* **322**, 413 (2008).

<sup>6</sup>M. Ternes, C. P. Lutz, C. F. Hirjibehedin, F. J. Giessibl, and A. J. Heinrich, *Science* **319**, 1066 (2008).

<sup>7</sup>S. Hirth, F. Ostendorf, and M. Reichling, *Nanotechnology* **17**, S148 (2006).

<sup>8</sup>R. Nishi, D. Miyagawa, Y. Seino, I. Yi, and S. Morita, *Nanotechnology* **17**, S142 (2006).

<sup>9</sup>F. J. Giessibl, S. Hembacher, H. Bielefeldt, and J. Mannhart, *Science* **289**, 422 (2000).

<sup>10</sup>L. Gross, F. Mohn, N. Moll, P. Liljeroth, and G. Meyer, *Science* **325**, 1110 (2009).

<sup>11</sup>D. Sawada, Y. Sugimoto, K. Morita, M. Abe, and S. Morita, *Appl. Phys. Lett.* **94**, 173117 (2009).

<sup>12</sup>Y. Sugimoto, I. Yi, K. Morita, M. Abe, and S. Morita, *Appl. Phys. Lett.* **96**, 263114 (2010).

<sup>13</sup>M. Ternes, C. González, C. P. Lutz, P. Hapala, F. J. Giessibl, P. Jelinek, and A. J. Heinrich, *Phys. Rev. Lett.* **106**, 016802 (2011).

<sup>14</sup>T. Arai and M. Tomitori, *Appl. Surf. Sci.* **188**, 292 (2002).

<sup>15</sup>T. Arai and M. Tomitori, *Appl. Surf. Sci.* **157**, 207 (2000).

<sup>16</sup>M. Guggisberg, M. Bammerlin, A. Baratoff, R. Lüthi, C. Loppacher, F. M. Battiston, J. Lü, R. Bennewitz, E. Meyer, and H. J. Güntherodt, *Surf. Sci.* **461**, 255 (2000).

<sup>17</sup>A. J. Weymouth, T. Wutscher, J. Welker, T. Hofmann, and F. J. Giessibl, *Phys. Rev. Lett.* **106**, 226801 (2011).

<sup>18</sup>T. Uda, H. Shigekawa, Y. Sugawara, S. Mizuno, H. Tochiwara, Y. Yamashita, J. Yoshinobu, K. Nakatsuji, H. Kawai, and F. Komori, *Prog. Surf. Sci.* **76**, 147 (2004).

<sup>19</sup>R. A. Wolkow, *Phys. Rev. Lett.* **68**, 2636 (1992).

<sup>20</sup>K. Sagisaka, D. Fujita, and G. Kido, *Phys. Rev. Lett.* **91**, 146103 (2003).

<sup>21</sup>K. Hata, S. Yasuda, and H. Shigekawa, *Phys. Rev. B* **60**, 8164 (1999).

<sup>22</sup>K. Sagisaka and D. Fujita, *Phys. Rev. B* **71**, 245319 (2005).

<sup>23</sup>Y. J. Li, H. Nomura, N. Ozaki, Y. Naitoh, M. Kageshima, Y. Sugawara, C. Hobbs, and L. Kantorovich, *Phys. Rev. Lett.* **96**, 106104 (2006).

<sup>24</sup>K. Sagisaka, D. Fujita, G. Kido, and N. Koguchi, *Surf. Sci.* **566–568**, 767 (2004).

<sup>25</sup>K. Sagisaka and D. Fujita, *Phys. Rev. B* **72**, 235327 (2005).

- <sup>26</sup>Y. Takagi, K. Nakatsuji, Y. Yoshimoto, and F. Komori, *Phys. Rev. B* **75**, 115304 (2007).
- <sup>27</sup>P. Jelinek, M. Svec, P. Pou, R. Perez, and V. Chab, *Phys. Rev. Lett.* **101**, 176101 (2008).
- <sup>28</sup>A. Sweetman, S. Jarvis, R. Danza, J. Bamidele, S. Gangopadhyay, G. A. Shaw, L. Kantorovich, and P. Moriarty, *Phys. Rev. Lett.* **106**, 136101 (2011).
- <sup>29</sup>D. Riedel, M. Lastapis, M. G. Martin, and G. Dujardin, *Phys. Rev. B* **69**, 121301 (2004).
- <sup>30</sup>See Supplemental Material at <http://link.aps.org/supplemental/10.1103/PhysRevB.84.085426> for additional information related to tunnel current related issues, imaging at zero bias, and dissipation during manipulation events.
- <sup>31</sup>F. J. Giessibl, *Rev. Mod. Phys.* **75**, 949 (2003).
- <sup>32</sup>F. J. Giessibl, *Appl. Phys. Lett.* **76**, 1470 (2000).
- <sup>33</sup>K. Morita, Y. Sugimoto, Y. Sasagawa, M. Abe, and S. Morita, *Nanotechnology* **21**, 305704 (2010).
- <sup>34</sup>A. Sweetman, S. Gangopadhyay, R. Danza, N. Berdunov, and P. Moriarty, *Appl. Phys. Lett.* **95**, 063112 (2009).
- <sup>35</sup>J. Soler, E. Artacho, J. Gale, A. Garcia, J. Junquera, P. Ordejon, and D. Sanchez-Portal, *J. Phys. Condens. Matter* **14**, 2745 (2002).
- <sup>36</sup>G. W. Brown, H. Grube, M. E. Hawley, S. R. Schofield, N. J. Curson, M. Y. Simmons, and R. G. Clark, *J. Appl. Phys.* **92**, 820 (2002).
- <sup>37</sup>S. R. Schofield, N. J. Curson, J. L. O'Brien, M. Y. Simmons, R. G. Clark, N. A. Marks, H. F. Wilson, G. W. Brown, and M. E. Hawley, *Phys. Rev. B* **69**, 085312 (2004).
- <sup>38</sup>R. J. Hamers, R. M. Tromp, and J. E. Demuth, *Phys. Rev. B* **34**, 5343 (1986).
- <sup>39</sup>K. Hata, Y. Sainoo, and H. Shigekawa, *Phys. Rev. Lett.* **86**, 3084 (2001).
- <sup>40</sup>Y. Naitoh, Y. J. Li, H. Nomura, M. Kageshima, and Y. Sugawara, *J. Phys. Soc. Jpn.* **79**, 013601 (2010).
- <sup>41</sup>L. Kantorovich and C. Hobbs, *Phys. Rev. B* **73**, 245420 (2006).
- <sup>42</sup>S. Morita, R. Wiesendanger, and E. Meyer, *Noncontact Atomic Force Microscopy*, 1st ed. (Springer, Science+Business Media LLC, NY, 2002).
- <sup>43</sup>Y. Yoshimoto and M. Tsukada, in *Proceedings of the 25th International Conference on the Physics of Semiconductors*, edited by N. Miura and T. Ando (Springer, Berlin, 2001), pp. 277–278.
- <sup>44</sup>A. J. Heinrich, C. P. Lutz, J. A. Gupta, and D. M. Eigler, *Science* **298**, 1381 (2002).
- <sup>45</sup>J. Stroschio and R. Celotta, *Science* **306**, 242 (2004).
- <sup>46</sup>M. Abe, Y. Sugimoto, O. Custance, and S. Morita, *Appl. Phys. Lett.* **87**, 173503 (2005).
- <sup>47</sup>P. Rahe, J. Schutte, W. Schniederberend, M. Reichling, M. Abe, Y. Sugimoto, and A. Kuhnle, *Rev. Sci. Instrum.* **82**, 063704 (2011).